NASA TECHNICAL MEMORANDUM

NASA TM X-73535

NASA TM X-73535

(NASA-TM-X-73535) CORE NOISE SOURCE DIAGNOSTICS ON A TURBOFAN ENGINE USING CORRELATION AND COHERENCE TECHNIQUES (NASA) 27 p HC A03/MF A01 CSCL 21E

N77-11053

Unclas G3/07 54570

CORE NOISE SOURCE DIAGNOSTICS ON A TURBOFAN ENGINE USING CORRELATION AND COHERENCE TECHNIQUES

by Allen Karchmer and Meyer Reshotko
Lewis Research Center
Cleveland, Ohio 44135

TECHNICAL PAPER to be presented at the
Ninety-second Meeting of the Acoustical Society of America
San Diego, California, November 16-19, 1976

CORE NOISE SOURCE DIAGNOSTICS ON A TURBOFAN ENGINE USING CORRELATION AND COHERENCE TECHNIQUES

by Allen Karchmer and Meyer Reshotko

Lewis Research Center

ABSTRACT

Fluctuating pressure measurements at several locations within the core of a turbofan engine were made simultaneously with far-field acoustic measurements. Correlation and coherence techniques were used to determine the relative amplitude and phase relationships between core pressures at these various locations and between the core pressures and far-field acoustic pressure. The results indicate that the combustor is a low-frequency source region for acoustic propagation through the core nozzle and out to the far-field. Specifically, it was found that the relation between source pressure and the resulting sound pressure involves a 180^{o} phase shift and an amplitude transfer function which varies approximately as frequency squared. This is shown to be consistent with a simplified model using fluctuating entropy as a source term.

E-8961

INTRODUCTION

In recent years much progress has been made in reducing noise from turbofan engines. It is possible, however, that further reductions of noise from the two primary engine sources, the fan and the turbulent exhause jet, may not result in significant overall engine noise reductions. A threshold, or floor, may be reached attributable to various internal or core-engine noise sources. In fact, there is much evidence, that under conditions of takeoff or approach, when the jet noise is reduced because of relative velocity effects, internal or core noise sources are already a major contributor to overall engine noise (ref. 1).

Most attempts to date to identify core noise sources in operating engines have been restricted to acoustic measurements made entirely outside the engine (refs. 2 and 3, for example). Several investigators, though, have combined both internal (at a few locations) and external measurements using correlation techniques (refs. 4 and 5). To the authors' knowledge, however, there have been no published attempts to measure comprehensively the fluctuating pressure field at a sufficient number of locations within an operating engine core to enable a systematic examination of the phase, amplitude, and time relationships between internal pressure signals. Together with simultaneous acoustic measurements outside the engine to provide information on the internal-external relationship between pressure signals, such a measurement program can provide valuable insight into the nature, source, and mechanisms of core noise.

At the Lewis Research Center a comprehensive core noise test program was conducted on a Lycoming YF-102 turbofan engine over a broad range of engine operating conditions. The present paper describes some of the results and preliminary conclusions drawn from source diagnostic efforts in this program.

ENGINE, INSTRUMENTATION, DATA PROCESSING

Engine and Test Arena

The test program was conducted on an AVCO-Lycoming YF-102 turbofan engine which has a bypass ratio of 6 and a rated thrust of 33 KN. This engine has a 1 m diameter fan and a core consisting of 7 axial compressor stages, 1 centrifugal compressor stage, a reverse-flow annular combustor, and a four-stage turbine. The exit diameter of the core nozzle was 42 cm and the engine was operated with a bellmouth inlet. A cutaway illustration of the engine is shown in figure 1.

All tests were conducted in an outdoor acoustic arena with a hard surface ground plane. The far-field microphone array consisted of sixteen 1.27 cm condenser microphones on a 30.5 m radius arc centered on the

exhaust plane of the core nozzle. The microphones were spaced 10^{o} apart from 10^{o} to 160^{o}, measured from engine inlet. All microphones were mounted at ground level to minimize problems associated with ground reflections, and were fitted with windscreens.

Test Conditions

Simultaneous internal (i.e., core) fluctuating pressure and far-field acoustic measurements were made at eight different fan speeds at approximately equal intervals between 30% and 95% of maximum speed (7600 rpm). The corresponding range of combustor temperatures and core jet exhaust velocities were from 810 K, 98 m/sec to 1375 K, 314 m/sec. The results from only a single operating condition (43% speed), a single far-field microphone (120^{o}), and selected internal locations are reported here. The results presented are considered representative of all the data taken over a broad range of operating conditions and microphone locations.

Internal Probes

The dynamic pressure measurements within the engine core were made simultaneously with the far-field measurements and at seven different locations, as shown in figure 2. Their number and locations were: two just downstream of the compressor exit about 2 cm apart; one at the combustor inlet; two within the annular combustor itself, both at the same axial location but separated 90^{o} circumferentially; and two within the core nozzle, one just downstream of the turbine at the nozzle entrance and one close to the nozzle exit plane.

The actual transducers used were conventional 0.635 cm condenser microphones with pressure response cartridges. To avoid direct exposure of the microphones to the severe environment within the core, they were mounted outside the engine and the fluctuating static pressure in the engine

core was communicated to the transducers by means of a "semi-infinite" acoustic waveguide.

A drawing of a typical probe is shown in figure 3. The microphone was flush mounted in the acoustic waveguide through a supporting block and housed in a pressure chamber. Attached to the block were a 5/8 cm diameter sensing tube on one end and a coil of tubing of the same diameter, 30 m long, on the other. The sensing tube of each probe was flush mounted as a static pressure tap at each of the various measuring locations within the engine core. A regulated nitrogen purge flow was maintained in the sensing line to protect the microphone from hot core gases. Static pressure was balanced across the microphone by means of a small vent hole connecting the pressure chamber and sensing line. Figure 4 is a schematic of a typical core probe installation.

Prior to the tests, the frequency and phase response of the probes, and the effect of the nitrogen purge flow on probe response were checked. The frequency and phase response was determined by comparison against a microphone identical to the one used in the probe using a symmetric placement with respect to the axis of a loudspeaker. The input to the loudspeaker was a signal from a white noise generator low pass filtered at 10 kHz.

The results indicated that the frequency response of the probes was flat within ±2 dB from 50 Hz to 1500 Hz. Similarly, the phase response of the probes was flat within about 5^{o} up to 1500 Hz after accounting for the phase lag associated with the length of the sensing tube of each particular probe. Between 1500 Hz and about 3500 Hz the response was generally flat within ±4 dB and $\pm 10^{o}$. Beyond 3500 Hz the response curves showed severe distortion. As will be shown later, though, with the exception of high frequency tones generated by the compressor and turbine (and not studied in the present work), the core noise associated with this engine was confined to a frequency range well within the acceptable response region of the probes. The pseudo-sound generated by the nitrogen purge flow through the probe was found to be a minimum of 20 dB below the core fluctuating pressure at the highest purge flow rate required in the engine tests.

Data Acquisition and Processing

The signals from the internal probes and far-field microphones were FM-recorded on magnetic tape in 2-minute record lengths for later processing. The internal probes and far-field microphones were calibrated with a pistonphone prior to and at the end of each day's running. Since the results and conclusions presented here are only concerned with the phase and time relationships between various pairs of signals, it was unnecessary to account for atmospheric absorption, corrections to standard day, etc.

The results given in this paper were obtained by off-line processing of the taped data on a two-channel fast Fourier transform digital signal processor with built-in a-d converters and 120 dB/octave anti-aliasing filters. The processor was capable of direct computation of up to 4096 ensemble averages of a 1024 point forward or inverse Fourier transform to yield either time-domain (correlation) or frequency domain (amplitude and phase spectra, transfer function, and coherence) information. The processor also permitted editing operations on a computed transform (e.g., time delay removal on correlation functions) and then Fourier inversion of the edited transform. This latter capability provided valuable information on the phase relationship between two signals separated in time.

EXPERIMENTAL RESULTS

Broadband Correlations

The normalized cross-correlation between pressure signals from the two tailpipe probes is shown in figure 5 (probes 6 and 7, fig. 2). Both signals were low-pass filtered at 1600 Hz prior to correlation. This cut-off frequency was chosen as the approximate upper limit of the acceptable response range of the probes. This was not a significant limitation since core noise is a relatively low frequency phenomenon except for tones

associated with rotating machinery. The two signals correlate rather strongly at a positive delay time of 0.55 msec. Considering the gas temperature (~670 K), flow velocity (~90 m/sec) and probe separation (0.34 m), the time for an acoustic wave to travel between the two probes is computed to be about 0.56 msec. The evidence suggests therefore, that the probes are detecting an acoustic signal.

The positive time delay in figure 5 indicates that the signal originates upstream of the tailpipe; hence it is natural to examine the relation between the signals from the combustor probe (4), and the tailpipe. The cross-correlations between the combustor probe signal and the upstream and downstream tailpipe probe signals are shown in figures 6(a) and (b), respectively. These are seen to be significantly different from that of figure 5. There are no clearly defined dominant peaks, and the shapes of these functions are considerably more complex than those of figure 5. These functions do not have, for example, the symmetry properties associated with pure propagation or convection (i.e., just time delay).

Coherence Functions

The preceding results can be further explored by examining the coherence function between the signals from two probes. The coherence function is analogous to the cross-correlation function, with the information being presented in the frequency domain. It is essentially a normalized cross spectrum and must have a value between zero and one, with low/high coherence at a particular frequency meaning low/high correlation at that frequency.

The coherence function between the combustor signal and the upstream tailpipe signal is shown in figure 7. There are clearly three distinct and separate regions of coherence: one between zero and 250 Hz; another between about 400 Hz and 600 Hz; and a third between 750 Hz and 950 Hz. Because these three regions of coherence are so distinct, it is worthwhile

to examine their relative significance insofar as combustor-associated far field noise is concerned.

Figures 8 and 9 show, respectively, the coherence function between the combustor probe and the downstream tailpipe probe signals and between the combustor probe and the 120° far-field microphone signals. Between the combustor and the downstream tailpipe, as shown in figure 8, the two higher-frequency regions of coherence are diminished significantly while the low frequency region remains. As seen in figure 9, the coherence between fluctuating combustor pressure and the far-field acoustic pressure is limited entirely to the low frequency region below 250 Hz.

From these results it is evident that the regions of fluctuating pressure coherence above 400 Hz seen in figure 7 are either not associated with sound or with a linear sound producing mechanism or, if they are due to sound, such sound is not radiating to the far field. Hence, for purposes of examining combustor-related noise in this engine, attention can be limited to frequencies below 250 Hz.

Low-Pass Correlations

It is now of interest to reexamine the cross-correlations shown in figure 6 for only the low frequency part of the signals. The cross-correlation functions between the filtered signals from the combustor and the upstream and downstream tailpipe probes are shown in figures 10(a) and (b), respectively. The signals were low-pass filtered at 240 Hz. Here the functions are better characterized than the broadband correlations shown in figure 6, with clearly defined negative peaks. The delay time to the negative peak in figure 10(a) is about 5.8 msec. Because of the complex flow path between these two stations their actual separation distance can only be estimated, from which the propagation time is computed as 0.9 msec and the convection time as 4.1 msec. Thus, the observed 5.8 msec delay time to the peak is much closer to a convection time than to an acoustic propagation time. However, because of the

negative peak, this correlation function cannot be identified as one associated with pure convection.

That the fluctuating combustor pressure is related to the far field sound only for frequencies below 250 Hz can be further verified by examining the correlation function between combustor pressure and the far-field signal. The broadband correlation between these two locations (up to 1600 Hz) is shown in figure 11(a), and the low-pass (below 240 Hz) correlation is shown in figure 11(b). There is virtually no significant difference between the two and they are almost identical in shape to the low-pass correlation between the combustor and the tailpipe (fig. 10), except for the time delay which in figure 11 corresponds to the acoustic propagation time to the far field.

Phase and Amplitude Relations

The shape of the correlation function is entirely determined by the amplitude relationship between the two signals and by that part of the phase relationship which is not due to time delay. Time delay causes a phase shift which is linear with frequency and which serves only to translate the correlation function. The phase shift between combustor and upstream tailpipe signals, as computed directly by the analyzer, is shown in figure 12(a) for the signals low-pass filtered at 240 Hz. The plot shows a phase shift between the two signals which is linear with frequency, and which is characteristic of the phase relationship between two signals with time delay between them. The phase difference unobscured by time delay was obtained by translating the peak of the filtered cross-correlation function in figure 10(a) to zero time delay by means of the editing feature on the analyzer and then computing the Fourier transform of the translated cross-correlation. The result of this computation is a complex function with real and imaginary parts which can be combined in polar form to produce amplitude (of the cross-spectrum) and phase.

The phase result is shown in figure 12(b). The result indicates a relatively constant 180° phase shift between the two (filtered) signals after time delay removal, over most of the frequency range considered.

An amplitude transfer function between the combustor and upstream tailpipe pressure signals can also be computed, and in conjunction with the phase information above uniquely determines the relationship between the two signals over the relevant frequency range. In the present context, this transfer function between the two signals is the ratio of the amplitude of the cross-spectrum to the amplitude of the auto-spectrum of the combustor pressure. The result of this computation is shown in figure 13. The transfer function varies approximately as frequency to the 1.7 power over most of the range considered (~5 dB/octave).

Between the two tailpipe stations, however, the pressure amplitude and phase relationships are different. Earlier it was suggested that the pressure signals detected by the two tailpipe probes were associated with an acoustic wave. This can be explored further by examination of the zero time delay phase shift and amplitude transfer function between the two stations. If only time delay prevails between the two tailpipe signals, then there should be a zero degree phase shift between the two signals after time delay removal, and the amplitude transfer function should be independent of frequency (i.e., flat). The phase difference between the two signals, over the 240 Hz low-pass frequency range, after time delay removal, is shown in figure 14. This result was obtained in the same manner as for figure 12(b). A zero degree phase shift independent of frequency is clearly evident. Similarly, the transfer function, shown in figure 15, is flat, with no frequency dependence.

That the acoustic signal which exists in the tailpipe does in fact radiate to the far field and contribute to overall engine noise can be seen in figures 16 through 18. The coherence function between downstream tailpipe pressure and the 120° far-field signal is shown in figure 16. Comparison of this figure with figure 9 (the coherence between combustor pressure and far-field) shows that although here there is an additional broad region of low coherence above about 250 Hz, the region of dominant coherence is below 250 Hz.

Figure 17 shows the phase difference between the downstream tailpipe pressure and 120° far field signal. This was obtained by Fourier

transforming the correlation function between the two signals (not shown) after removal of the time delay as described previously. The result is clearly a zero-degree phase shift over most of the frequency range of interest. The corresponding amplitude transfer function is shown in figure 18, and it is seen to be a relatively flat function. These two characteristics of the data, flat transfer function and zero degree phase shift after removal of the time delay, indicate that only a time delay exists between the two signals. This, combined with a measured delay time corresponding to the time for sound to travel between the two positions, indicates pure acoustic propagation.

To complete the picture, the phase and amplitude relations between combustor and far-field pressures are shown in figures 19 and 20. Figure 19 shows the phase shift between combustor pressure and the 120° far-field microphone, after time delay removal. It was computed by removing the time delay from the cross-correlation shown in figure 11(b) and Fourier transforming the result. Once again, it is seen that there is essentially a 180° phase shift over the frequency range of interest. The amplitude transfer function is shown in figure 20. As in figure 13, the transfer function varies with frequency approximately to the 1.7 power over most of the range considered.

Concluding Remarks on Experimental Results

The experimental results can be summarized as follows. The fluctuating pressure in the combustor correlates with the far-field sound only at frequencies below 250 Hz, with the peak occurring near 125 Hz. Within this frequency range the combustor pressure is related to the fluctuating tailpipe pressures through a 180° phase shift and a relative amplitude change dependent on frequency to the 1.7 power. The pressure signal detected within the tailpipe is identified as being acoustic, and is shown to radiate, and thereby contribute, to the far-field. Between combustor and upstream tailpipe stations, although the time delay corresponds approximately to a convecting disturbance, it cannot be identified as such because

of the phase and amplitude relationship between the two. Finally, between the combustor and far-field, the 180^{o} phase shift and the variation with frequency to the 1.7 power also prevails.

From these results it is concluded that the combustor probe is located in a source region for far-field sound at frequencies below 250 Hz. Somewhere between the combustor and the upstream tailpipe position, the pressure disturbance becomes the source of acoustic energy which propagates through the tailpipe and out to the far-field.

ANALYTICAL CONSIDERATIONS

The relationship between the fluctuating pressure in the source region and the far-field acoustic pressure involves a 180^{o} phase shift and relative amplitude increase dependent on frequency to the 1.7 power. The nature of this relationship may be formalized by recalling that differentiation in the time domain corresponds to multiplication by frequency in the frequency domain. Further, a single time derivative of a signal results in a phase shift of 90^{o} in the derived signal. Hence a phase shift of 180^{o} and a multiplication by frequency squared in the frequency domain is equivalent to two time derivatives. In the present case, then, the combustor related far-field pressure behaves approximately as the 2nd time derivative of the fluctuating combustor pressure.

A physical basis for this can be shown through an admittedly simplified model of a Lighthill type formulation. Lighthill related the fluctuating density in an acoustic radiation field to fluid mechanical stresses in a source region as follows (see ref. 6, for example):

$$\rho'(\bar{X},t) = \frac{1}{4\pi x c_o^4} \int \frac{\partial^2}{\partial t^2} T_{ij}\left(\bar{Y}_o + \bar{\eta}, t - \frac{r}{c_o}\right) d^3\bar{\eta} \qquad (1)$$

where

ρ' is the fluctuating density

$\bar{X}$ is the position vector of a point in the radiation field

$\bar{Y}_o + \bar{\eta} = \bar{Y}$ is the position vector of a point in the source region

$x = |\bar{X}|$

$r = |\bar{X}-\bar{Y}|$

c_o is the speed of sound

T_{ij} is Lighthill's turbulence stress tensor:

$$T_{ij} \equiv \rho_o v_i v_j + \delta_{ij}\left(p' - c_o^2 \rho'\right) - e_{ij}$$

For the usual aeroacoustic sources, the procedure is to neglect the viscous stress tensor e_{ij} and assume that the source region is essentially isentropic so that $p' \approx c_o^2 \rho'$, where p' is the fluctuating pressure. The Reynolds stress term, $\rho_o v_i v_j$, is then retained as the only source term. In a region of combustion, however, it is not unreasonable to neglect the Reynolds stress term and retain $p' - c_o^2 \rho'$ as a measure of the fluctuating entropy, and hence as a source term.

Making the usual assumption that in the radiation field $p' \approx c_o^2 \rho'$ eq. (1) becomes

$$p'(\bar{X}, t) = \frac{1}{4\pi x c_o^2} \int \frac{\partial^2}{\partial t^2} S'\left(\bar{Y}_o + \bar{\eta}, t - \frac{r}{c_o}\right) d^3\bar{\eta} \qquad (2)$$

where $S' = p' - c_o^2 \rho'$ is the fluctuating entropy.

Forming a correlation function between the fluctuating pressure in the source region, $p'(\bar{Y}_o, t)$, and the fluctuating pressure in the radiation field, eq. (2) becomes

$$\overline{p'(\bar{Y}_o, t)p'(\bar{X}, t+\tau)} \propto \int \overline{p'(\bar{Y}_o, t) \frac{\partial^2}{\partial t^2} S'(\bar{Y}_o + \bar{\eta}, t+\tau)}\, d^3\bar{\eta} \qquad (3)$$

with the usual assumption that differences in retarded time $(t - r/c_o)$ can be neglected. The overbar indicates a time average. The integrand on the right hand side of eq. (3) is the correlation between a function and the 2nd derivative of another function, delayed in time.

A theorem relating correlations of jointly stationary random functions to their derivatives can be found in reference 7. It is expressed as

$$\overline{\frac{d^m}{dt^m} f_1(t) \frac{d^n}{dt^n} f_2(t+\tau)} = (-1)^m \frac{d^{n+m}}{d\tau^{n+m}} \overline{f_1(t) f_2(t+\tau)}$$

So eq. (3) can be written

$$\overline{p'(\bar{Y}_o, t) p'(\bar{X}, t+\tau)} \propto \frac{\partial^2}{\partial \tau^2} \int \overline{p'(\bar{Y}_o, t) S'(\bar{Y}_o + \bar{\eta}, t+\tau)}\, d^3\bar{\eta} \qquad (4)$$

Arbitrarily defining a correlation volume as

$$V_{corr} \equiv \frac{\int \overline{p'(\bar{Y}_o, t) S'(\bar{Y}_o + \bar{\eta}, t+\tau)}\, d^3\bar{\eta}}{\overline{p'(\bar{Y}_o, t) S'(\bar{Y}_o, t+\tau)}}$$

eq. (4) becomes

$$\overline{p'(\bar{Y}_o, t) p'(\bar{X}, t+\tau)} \propto V_{corr} \frac{\partial^2}{\partial \tau^2} \overline{p'(\bar{Y}_o, t) S'(Y_o, t+\tau)} \qquad (5)$$

The quantity which was measured in the experiment is the correlation on the left-hand side of eq. (5). From eq. (5), this must have the same shape as the 2nd derivative of a single point cross-correlation between pressure and entropy fluctuations. If these latter two are in phase, the 2nd derivative operation will result in a 180^o phase shift and frequency

squared relation between the two pressures on the left-hand side of eq. (5). The correlation on the right hand side of eq. (5) can be expanded as:

$$\overline{p'(\bar{Y}_o,t)S'(\bar{Y}_o,t+\tau)} \equiv \overline{p'(\bar{Y}_o,t)\left[p'(\bar{Y}_o,t+\tau) - c_o^2\rho'(\bar{Y}_o,t+\tau)\right]}$$

$$= \overline{p'(Y_o,t)p'(Y_o,t+\tau)} - \overline{p'(Y_o,t)c_o^2\rho'(Y_o,t+\tau)} \qquad (6)$$

In the first correlation on the right hand side of eq. (6) the pressure, of course, is in phase with itself. Hence, if the fluctuating pressure and density in the 2nd correlation are in phase (or the 2nd correlation makes a negligible contribution to the right hand side), the pressure and entropy fluctuations will be in phase, and the 180° phase shift and a frequency squared relationship will prevail in the frequency domain version of eq. (5).

CONCLUDING REMARKS

A measurement of the coherence spectrum between a fluctuating static pressure probe in the combustor of a turbofan engine and a microphone in the far-field indicated a linear relationship between the two pressures only at frequencies below about 250 Hz. Using this as a guide for computing filtered correlation functions, it was found that the combustor behaves as a source region for acoustic propagation through the tailpipe and out to the far field. Thus it has been shown that for this engine, at the condition tested, the combustor is a source of core noise, but its contribution is limited to frequencies below 250 Hz.

The relationship between source pressure and the resulting sound pressure was found to involve a 180° phase shift and an amplitude transfer function that varied as the 1.7 power of frequency. This was determined by removing the time delay associated with the filtered correlation functions and Fourier transforming the result. If the sound pressure were related to the source pressure by a 180° phase shift and a frequency-squared amplitude

dependence, this would correspond to a 2nd time derivative of the local source pressure. A simplified model using fluctuating entropy as a source term was shown to be consistent with this behavior. There are a number of possible reasons as to why an exponent of 1.7 on frequency was measured as compared to a theoretical exponent of 2. The most likely explanation is contamination of the acoustic signal in the far field by noise from other sources (possibly tailpipe scrubbing noise) which also correlate with fluctuating combustor pressure in the low frequency range. Another possible explanation is simply that the analysis in the previous section is not very rigorous. The correlation volume in eq. (5), for example, is not a constant and may be frequency dependent.

It should be mentioned that although the results from only a single operating condition and far-field microphone location were discussed in this paper, data for other engine operating conditions were also examined. The preliminary results from those tests appear to indicate that the strength of the correlation between fluctuating combustor pressure and far-field pressure varies only slightly with microphone angle. It was found, however, that the contribution of the combustor to overall engine noise decreases rapidly with increasing engine speed as the jet mixing noise becomes dominant.

REFERENCES

1. J. R. Stone, "On the Effects of Flight on Jet Engine Exhaust Noise," presented at the 90th Meeting of the Acoustical Society of America, San Francisco, Calif. (1975); see also NASA TM X-71819 (1975).

2. R. G. Hoch, P. Thomas, and E. Weiss, "An Experimental Investigation of the Core Engine Noise of a Turbofan Engine," AIAA Paper No. 75-526 (Mar. 1975).

3. R. P. Gerend, H. A. Kumasaka, and J. P. Roundhill, "Core Engine Noise," AIAA Paper No. 73-1027 (Oct. 1973).

4. D. C. Mathews, and A. A. Peracchio, "Progress in Core Engine and Turbine Noise Technology," AIAA Paper No. 74-948 (Aug. 1974).

5. E. A. Burdsall, F. P. Brochu, and V. M. Scaramella, "Results of Acoustic Testing of the JT8D-109 Refan Engines," Pratt & Whitney Aircraft, PWA-5298, NASA CR-134875 (1975).

6. M. E. Goldstein, "Aeroacoustics," NASA SP-346 (1974), p. 113.

7. A. Papoulis, Probability, Random Variables, and Stochastic Processes (McGraw-Hill Book Company, New York, 1965), p. 317.

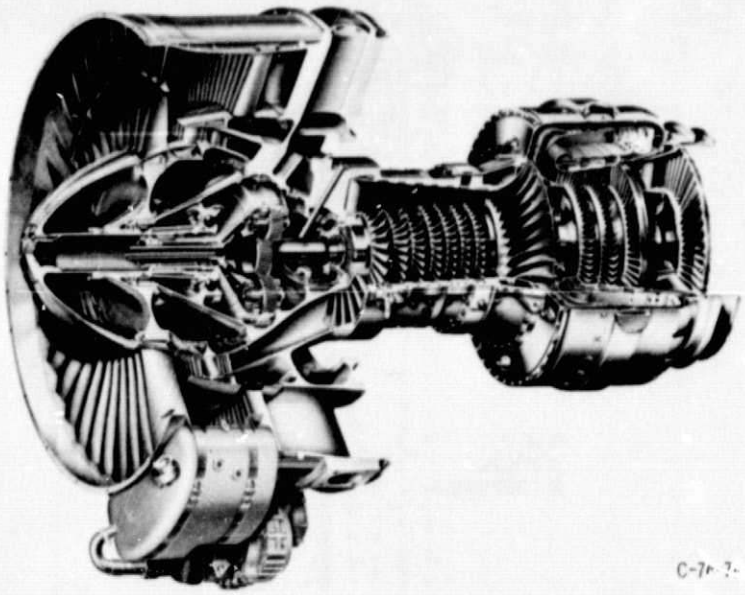

Figure 1. - Cutaway illustration of YF-102.

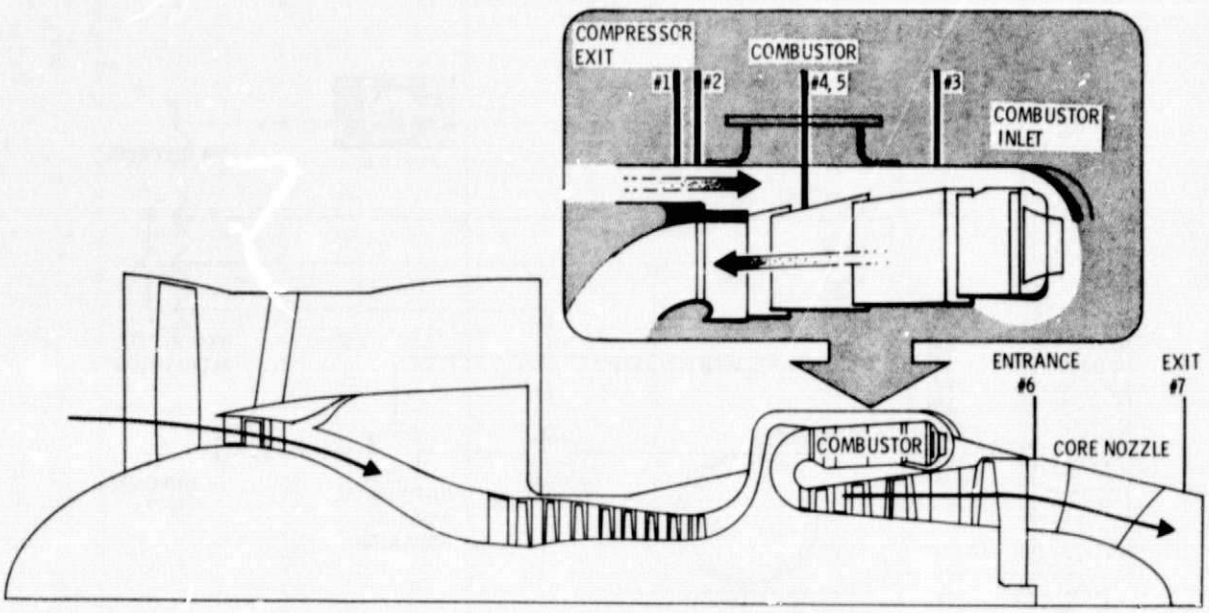

Figure 2. - Core pressure probe locations.

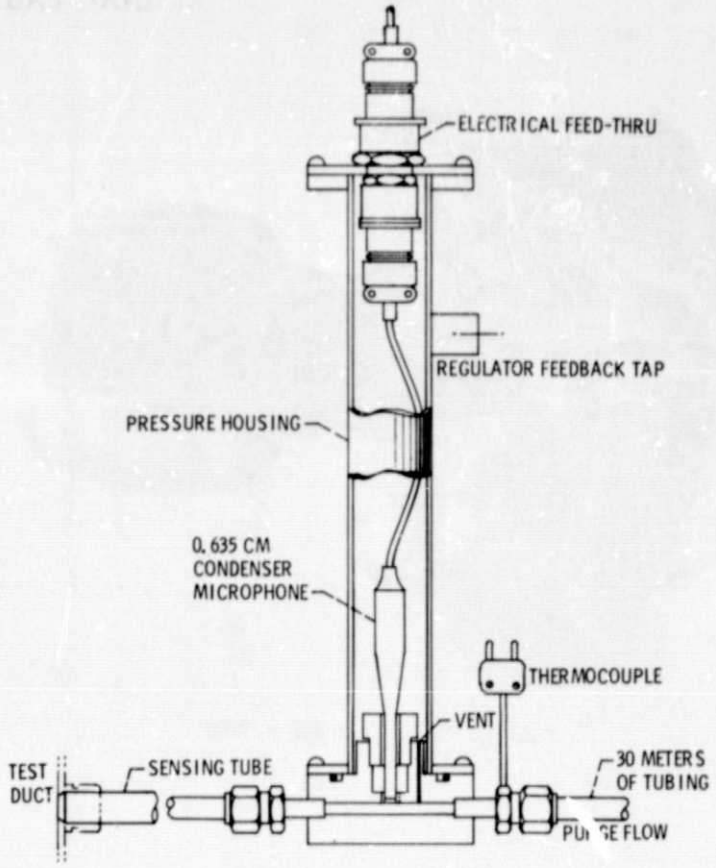

Figure 3. - Core pressure probe.

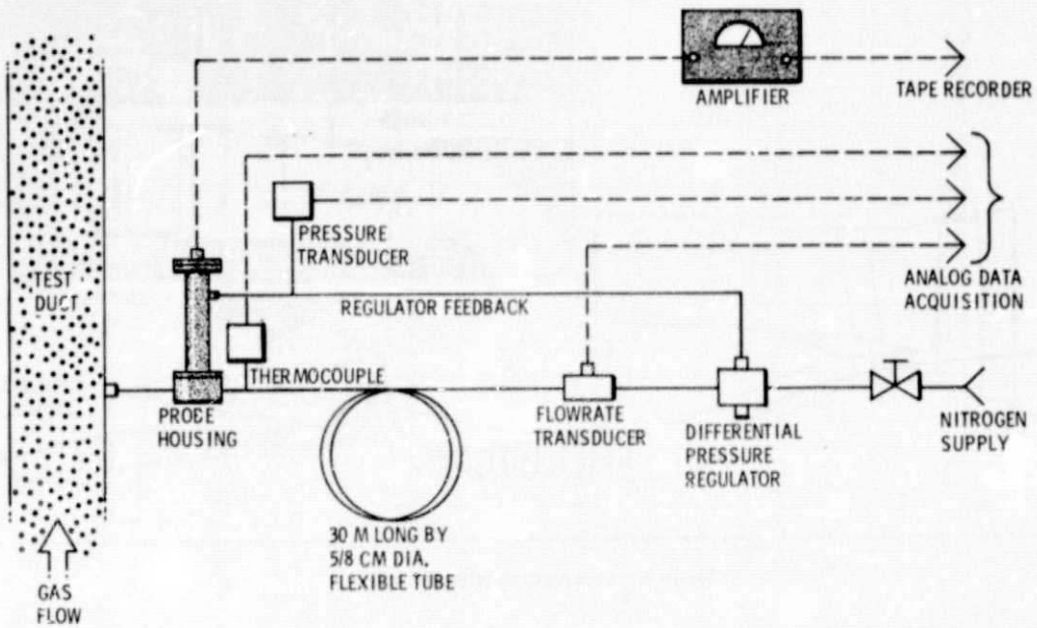

Figure 4. - Schematic of core probe installation.

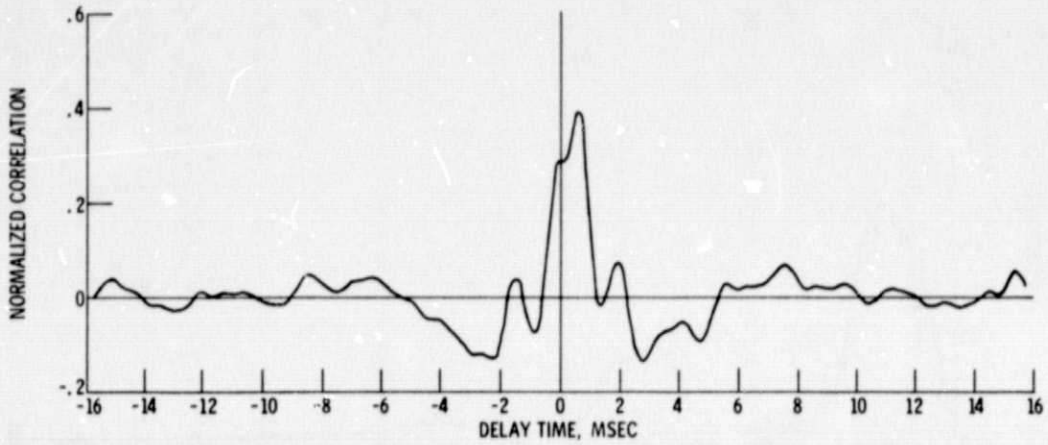

Fig. 5. - Cross-correlation between tailpipe pressures; data low-pass filtered at 1600 Hz.

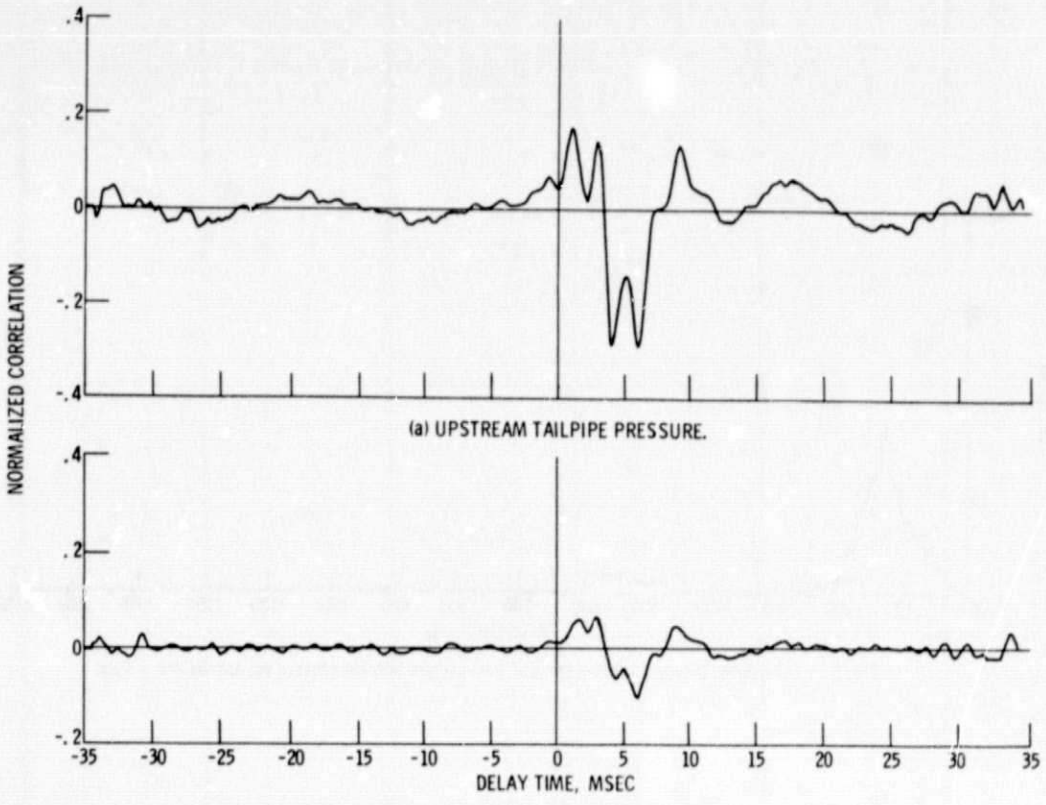

Fig. 6. - Cross-correlation between combustor pressure and tailpipe pressures; data low pass filtered at 1600 Hz.

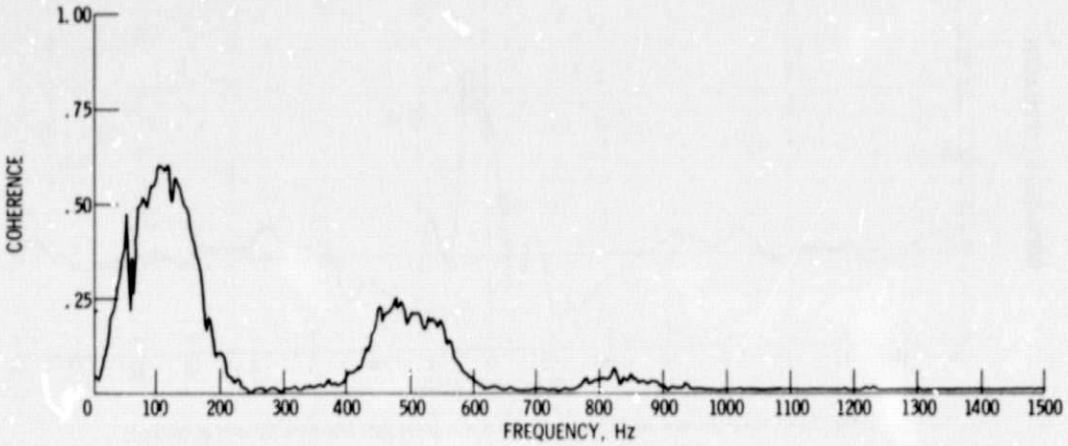

Fig. 7. - Coherence between combustor and upstream tailpipe pressures; bandwidth = 3 Hz.

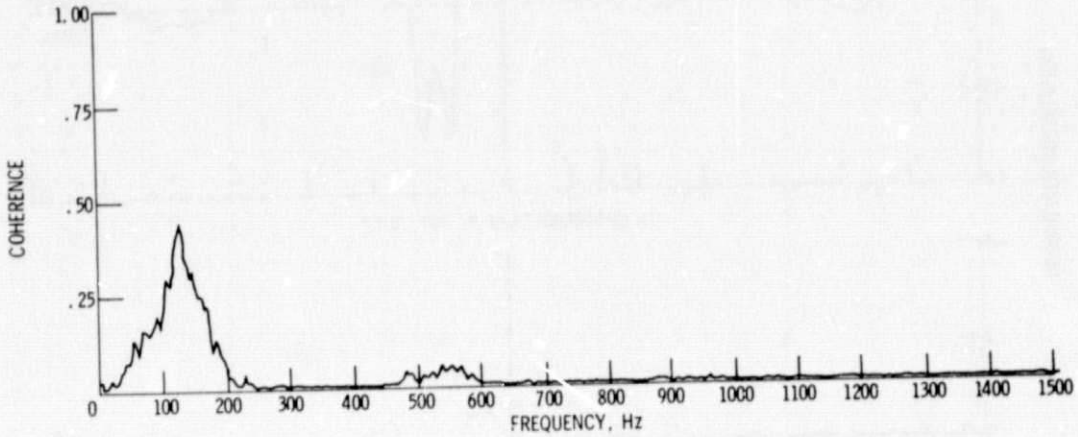

Fig. 8. - Coherence between combustor and downstream tailpipe pressures; bandwidth = 3 Hz.

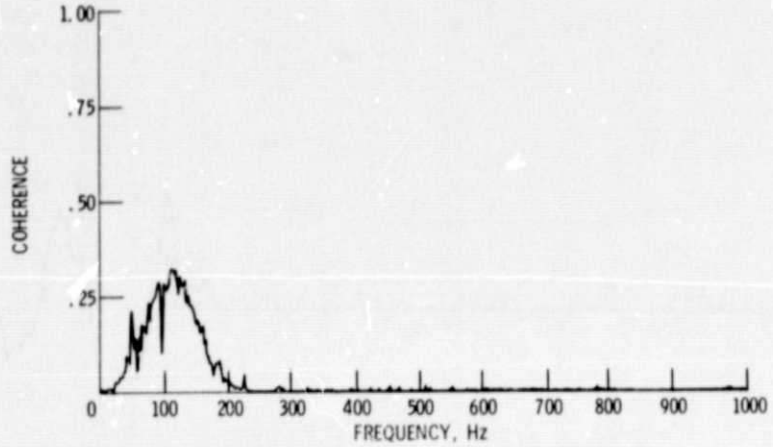

Fig. 9. - Coherence between combustor pressure and 120° far-field pressure; bandwidth = 2 Hz.

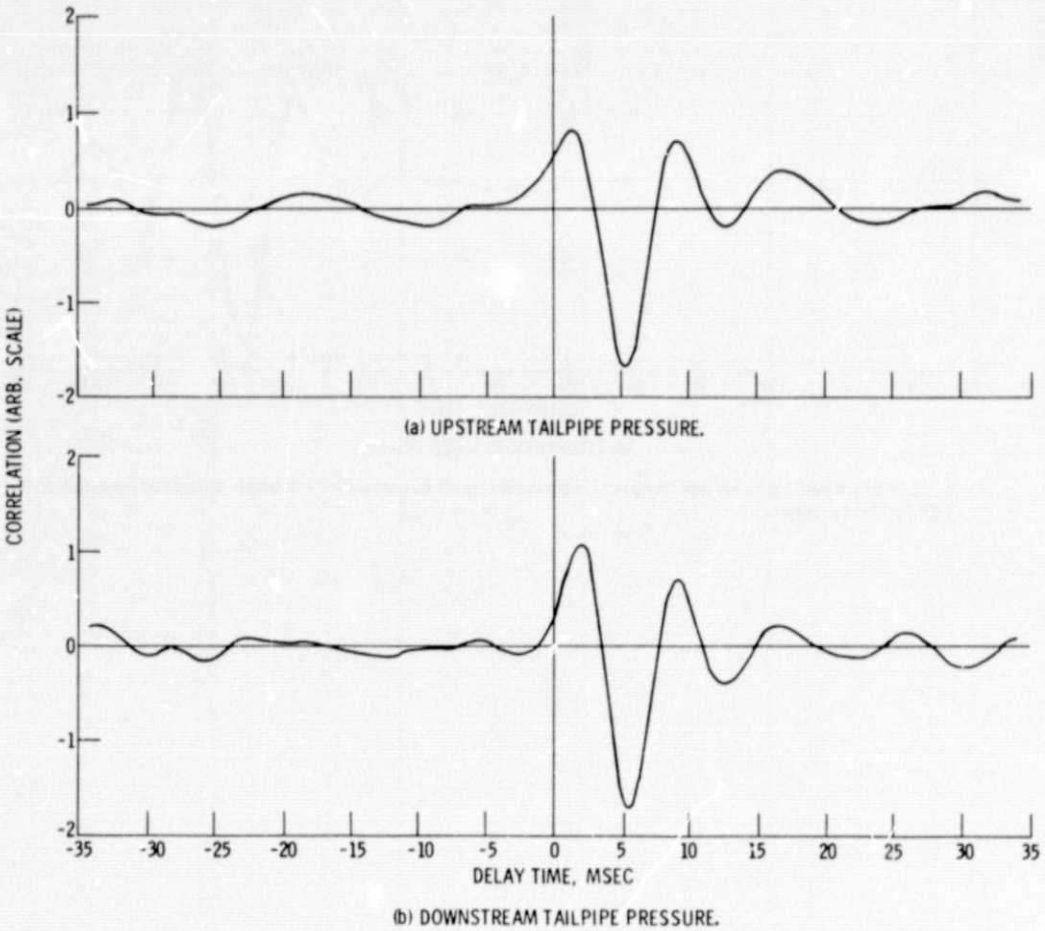

Fig. 10. - Low-pass filtered cross-correlation between combustor and tailpipe pressures; data low pass filtered at 240 Hz.

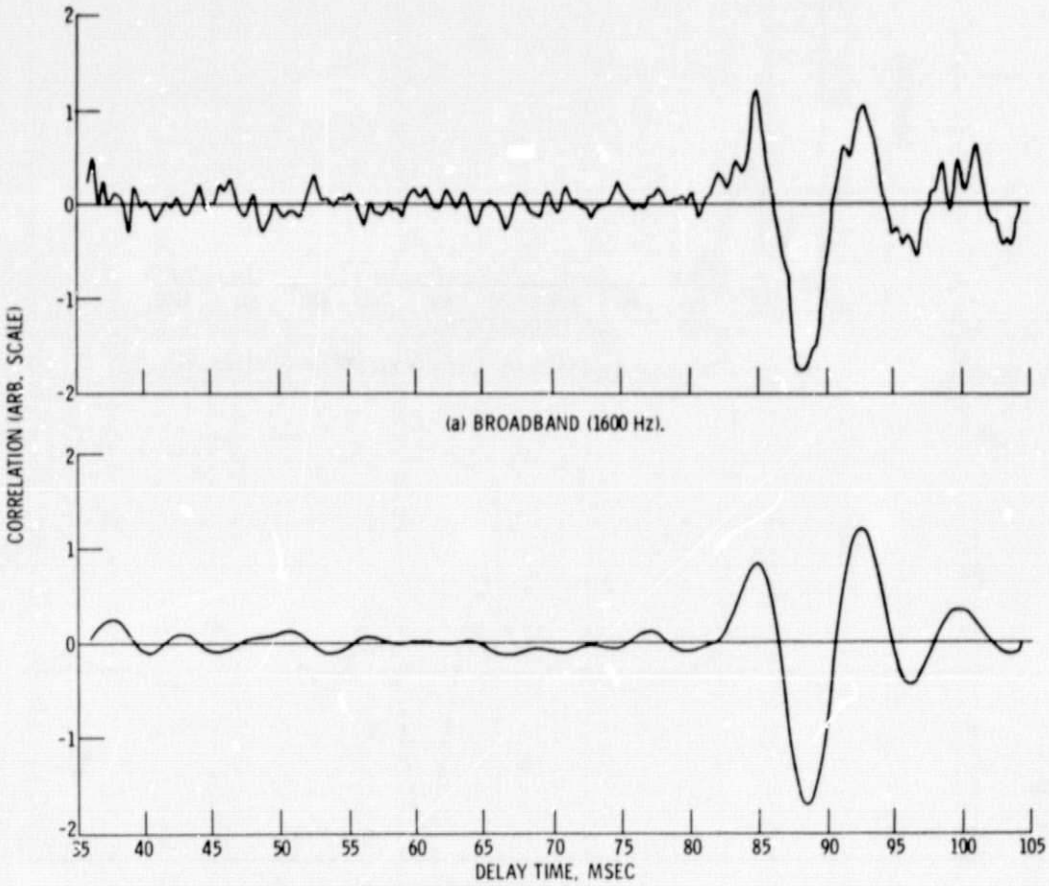

Fig. 11. - Broadband (1600 Hz) and low-pass filtered (240 Hz) cross-correlations between combustor pressure and 120^0 far-field pressure.

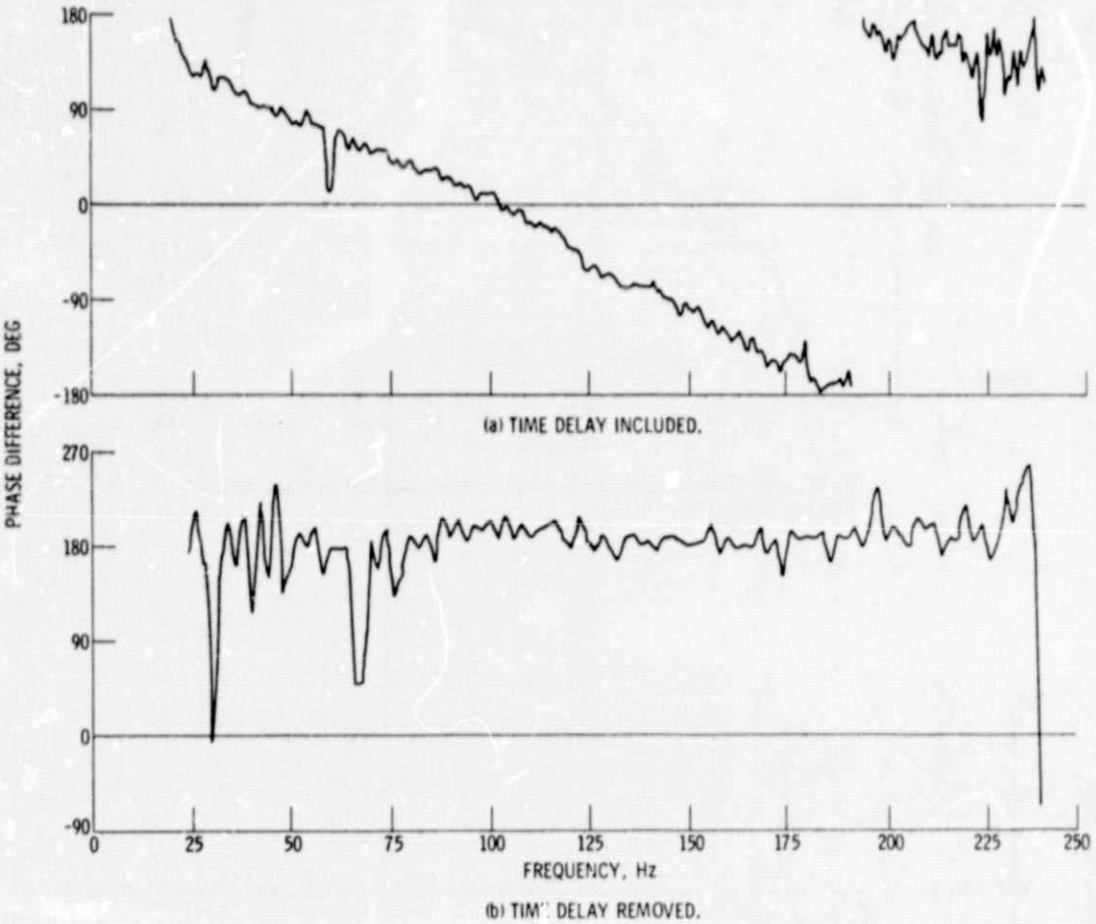

Fig. 12. - Phase shift between combustor and upstream tailpipe pressures; bandwidth = 0.6 Hz.

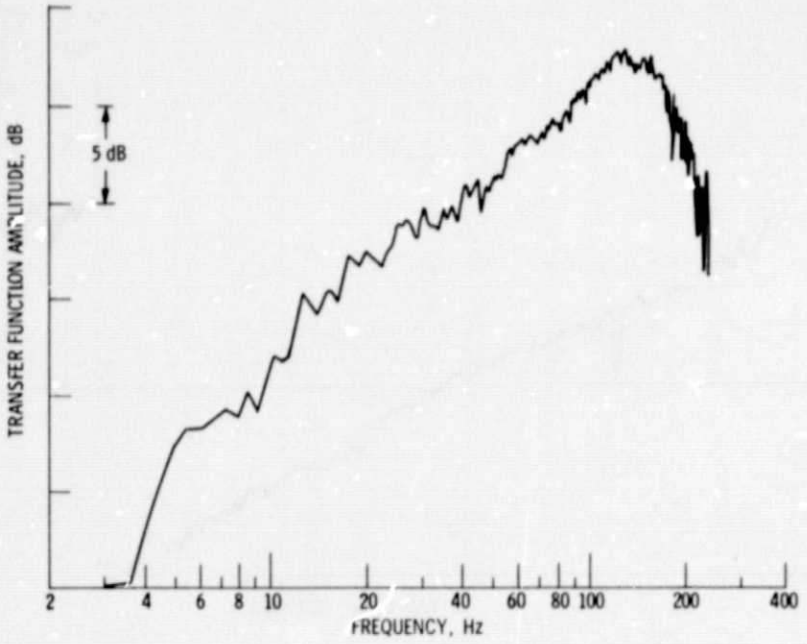

Fig. 13. - Amplitude transfer function between combustor and upstream tailpipe pressures; bandwidth = 0.6 Hz.

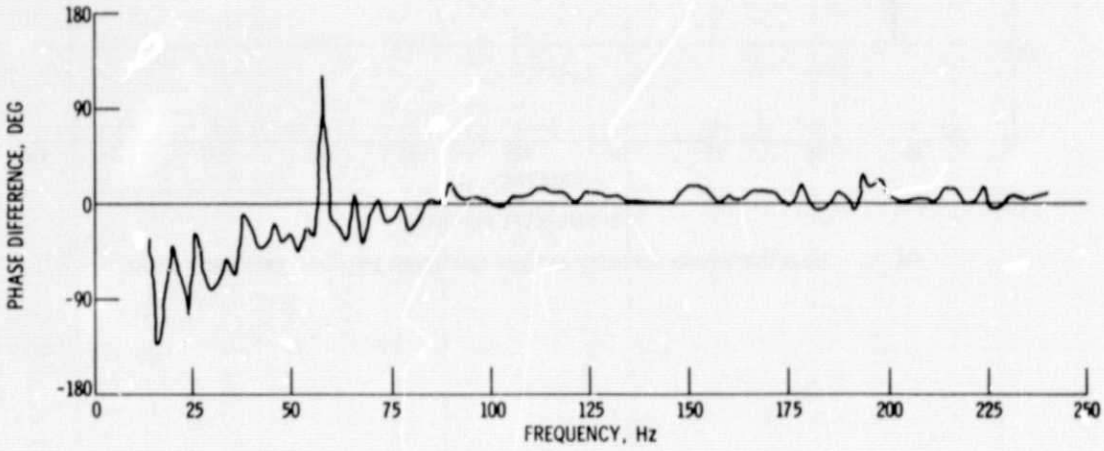

Fig. 14. - Phase shift between upstream and downstream tailpipe pressures; time delay removed; bandwidth = 0.6 Hz.

E-8961

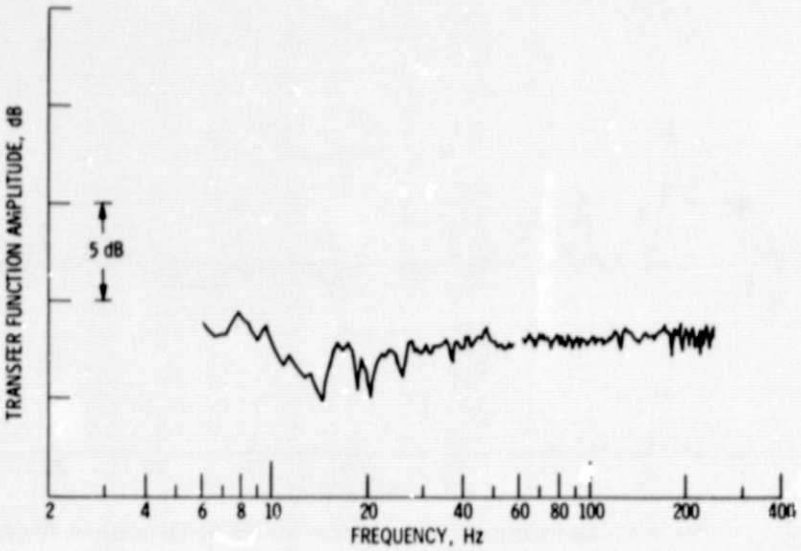

Fig. 15. - Amplitude transfer function between upstream and downstream tailpipe pressures; bandwidth = 0.6 Hz.

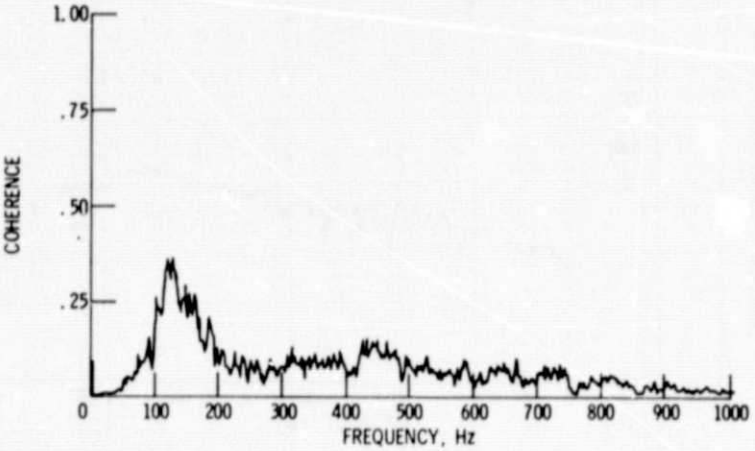

Fig. 16. - Coherence between downstream tailpipe pressure and 120° far-field microphone; bandwidth = 2 Hz.

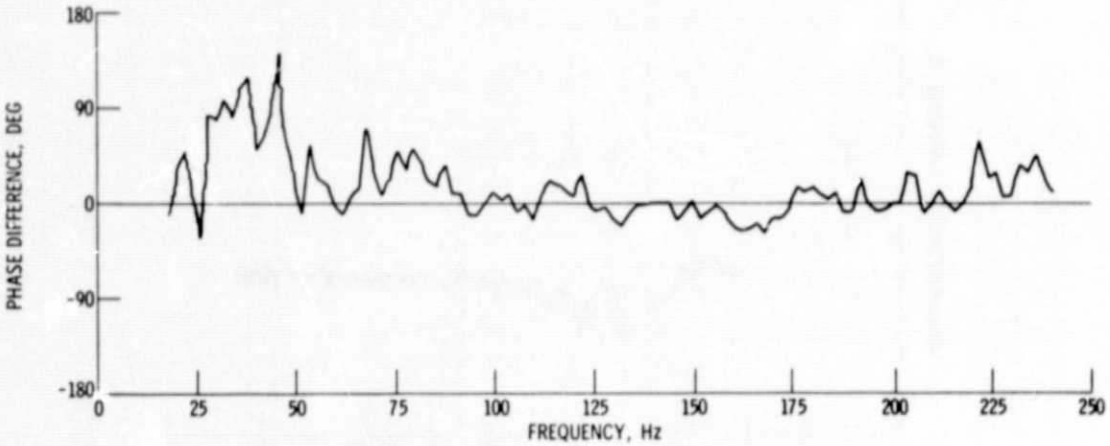

Fig. 17. - Phase shift between downstream tailpipe pressure and 120° far-field pressure; time delay removed; bandwidth = 0.6 Hz.

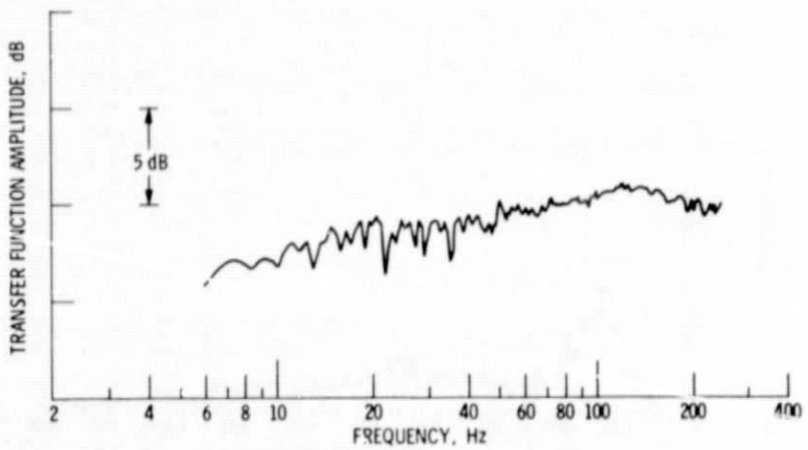

Fig. 18. - Amplitude transfer function between downstream tailpipe pressure and 120° far-field pressure; bandwidth = 0.6 Hz.

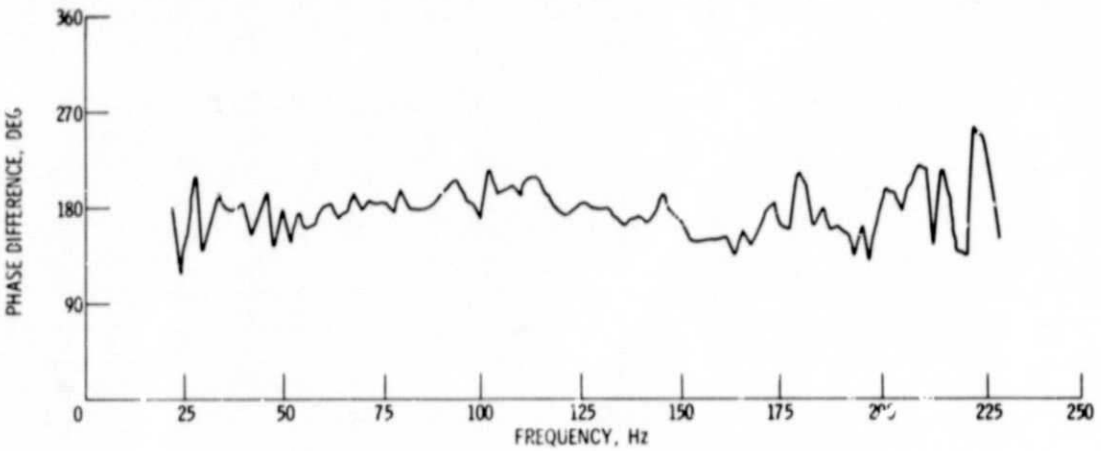

Fig. 19. - Phase shift between combustor pressure and 120° far-field pressure; time delay removed; bandwidth = 2.0 Hz.

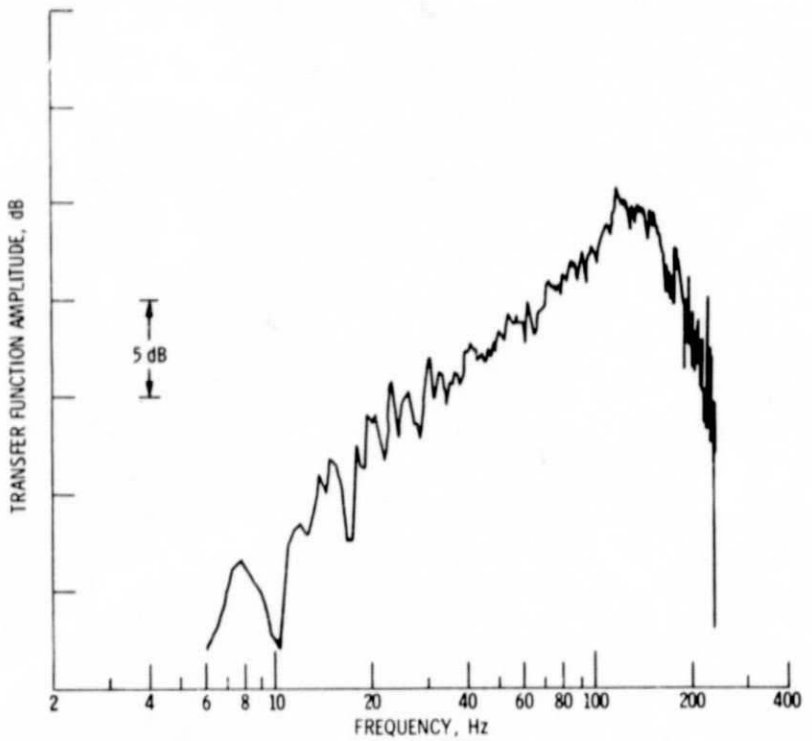

Fig. 20. - Amplitude transfer function between combustor pressure and 120° far-field pressure; bandwidth = 0.6 Hz.